Available online at www.sciencedirect.com
SCIENCE DIRECT®
Journal of Organometallic Chemistry 690 (2005) 2017–2026
Journal of Organometallic Chemistry
www.elsevier.com/locate/jorganchem

# Novel cyclometallated Pd(II) and Pt(II) complexes with indole derivatives and their use as catalysts in Heck reaction

Giancarlo Cravotto [a], Francesco Demartin [b], Giovanni Palmisano [c], Andrea Penoni [c,*], Tiziano Radice [c], Stefano Tollari [c,*]

[a] *Dipartimento di Scienza e Tecnologia del Farmaco, Università degli Studi di Torino, via Giuria 9, 10125 Torino, Italy*
[b] *Dipartimento di Chimica Strutturale e Stereochimica Inorganica, Università degli Studi di Milano, Via Venezian 21, 20133 Milano, Italy*
[c] *Dipartimento di Scienze Chimiche ed Ambientali, Università degli Studi dell'Insubria, via Valleggio 11, 22100 Como, Italy*

Received 26 November 2004; accepted 26 November 2004

**Abstract**

Several palladacycle and platinacycle complexes have been prepared from easily available or naturally occurring indole derivatives, such as gramine and related compounds. Dimeric complexes were obtained with $Pd(OAc)_2$, while $Pt(DMSO)_2Cl_2$ mainly afforded monomeric structures. A notable feature of these reactions was the formation of new M–C bonds between Pd or Pt and C-2 and C-3 of the indole ring. With ligands like 2-(2′-pyridyl)-1*H*-indoles, N–N metallacycles were generated instead: in fact new C–M bonds with the C-3 position could only form if *N*-substituted indoles were used. The reactivity of Pd dimeric complexes with $PPh_3$, *sym*-collidine and DMAP was explored to obtain monomeric complexes. Three such compounds were prepared, one of which was characterized by X-ray diffraction. Metathetical reactions were carried out to effect a ligand exchange replacing OAc with halide ions, with the aim to synthesize μ-Cl and μ-Br bridged structures. Turning to the synthesis of hetaryl complexes, functionalization of the C-2 position on the indole ring was achieved. These complexes were prepared by substitution reactions starting from gramine and/or its alkylammonium salts.


*Keywords:* Indole derivatives; Metallacycles; Palladium; Platinum; Catalysis; Heck reaction

## 1. Introduction

Intramolecular activation of C–H bonds through the agency of transition metal ions (cyclometallation), first described by Kleiman and Dubeck [1], has attracted much interest in the last two decades. Many useful applications of cyclometallated compounds in organic chemistry are well established, e.g., to the synthesis of heterocycles and of enantiomerically enriched molecules, to prepare liquid crystals (metallomesogens) [2], to the resolution of racemates and to the evaluation of optical purity [3]. Finally, they have proved useful in the design of molecules with promising photochemical [4] and anticancer properties [5]. Cyclometallated compounds are organometallic complexes embodying an E–M–C connectivity of σ-bonds, where E is a heterodonor atom of the 15- or 16-group, M a metallic atom and C a carbon donor. They are usually classified according to the metal, the donor atom(s) or chelate ring size. Cyclopalladated compounds with a variety of N-donor ligands (e.g., amines, azobenzenes, imines [6], hydrazones [7], oximes and N-centered hetarenes) have been extensively investigated. Whereas heteroatom-directed cyclometallation of benzenoids and hetarenes is well known, the chemistry of the analogous indole derivatives remains partially unexplored [6–11]. In this

* Corresponding authors. Tel.: +390312386471; fax: +390312386449.
*E-mail address:* stefano.tollari@uninsubria.it (S. Tollari).

0022-328X/$ - see front matter © 2004 Elsevier B.V. All rights reserved.
doi:10.1016/j.jorganchem.2004.11.042

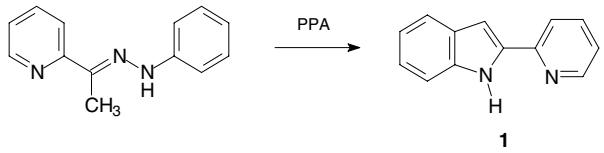


Scheme 1.

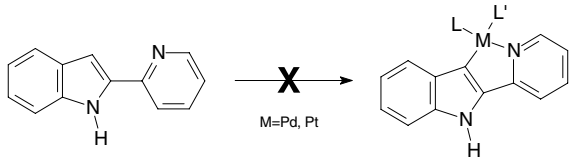


Scheme 2.

context we are currently studying the structures and physico-chemical properties of 5- and 6-membered metallacycles containing an indole subunit with a tethered N-donor group [8–11]. In particular we have focused our interest on complexes of Pt(II) and Pd(II) with variously substituted bidentate [C, N] amines and imines as well as tridentate [C, N, O] hydrazones. The present work examined the formation of Pd(II) and Pt(II) complexes with 2-(2-pyridyl)-1*H*-indole ($HL^1$) **1** and their performance as precatalysts in the Heck reaction between iodobenzene and *tert*-butylacrylate. **1** was prepared in excellent yield by Fischer indolization [12] of 2-acetylpyridine with phenylhydrazine in polyphosphoric acid (PPA) at 150 °C (Scheme 1).

The juxtaposition of a pyridine and an indole system, presenting two potential donor sets (i.e., N,N or C,N) in a 1,4-relationship is particularly interesting. Pyridine behaves as a π-deficient system with Lewis basicity while indole is a π-excessive system $10e^-$ system with a good H-bond donor atom. When we used **1** as ligand for the synthesis of cyclometallated compounds with the aim to generate a new C–M bond, we found that **1** behaves exclusively as a nitrogen chelating agent, forming a N–M–N coordination compound.

Ligand **1** could, in principle, behave as an ambident nucleophile (N-1 vs. C-3) although normally indoles prefer electrophilic substitution (e.g., cyclometallation) at C-3, the 1-position being clearly less reactive. The reaction in degassed EtOH of **1** with $Li_2[PdCl_4]$ in the presence of NaOAc as a proton scavenger (room temperature, 2 h) afforded the orange $[(L^1\text{-N,N})\ Pd(\mu\text{-Cl})]_2$ complex **2** exhibiting N,N ligation, whose structure was supported by elemental analysis and IR spectroscopy. The absence of the two bands at 3100 and 3010 $cm^{-1}$ attributed to the $\nu_{(N-H)}$ mode of the ligand indicated that **1** had been deprotonated and coordinated in the amido (indolato) form (Scheme 2).

Complex **2** was uneventfully converted to the bromo-bridged analogue, $[(L^1\text{-N,N})\ Pd(\mu\text{-Br})]_2$ **3** by metathetical reaction with LiBr in MeOH at room temperature. On the other hand, the reaction of **1** with equivalent amounts of $Pd(OAc)_2$ in dichloromethane at room temperature (1 h) produced the dimeric acetate complex $[(L^1\text{-N,N})\ Pd(\mu\text{-OAc})]_2$ **4** (Scheme 3). Strong bands were observed at 1572, 1412 $cm^{-1}$ due to $\nu_{as\ (COO)}$ and $\nu_{s\ (COO)}$, values consistent with a bridged acetate ligand; in $^1H$ NMR spectra the singlet resonance at 2.35 ppm (6H) was assigned to the magnetically equivalent Me acetate groups, in accord with a *trans* geometry of the [N^N] cyclometallated compound **4**.

Complex **5** $[(L^1\text{-N,N})\ Pd(DMAP)(OAc)]$ was isolated after the addition to complex **4** of 4-dimethylaminopyridine (DMAP) in $CH_2Cl_2$. The $^1H$ NMR spectrum of **5** was unexceptional. Pale yellow crystals suitable for single-crystal X-ray structure determination were obtained by vapour diffusion of $Et_2O$ into a $CH_2Cl_2$ solution of the crude product. **5** was then fully characterized by X-ray diffraction. Likewise complex **4** could be reacted with the appropriate ligating species to give **6** and **7**. A sample of **4** placed in an NMR tube was treated at room temperature in $CDCl_3$ with 1 equiv. of triphenylphosphine or 2,4,6-trimethylpyridine (*sym*-collidine), whereupon an instantaneous reaction took place to give the corresponding $[(L^1\text{-N,N})\ Pd\ L(OAc)]$ complexes **6** and **7**, respectively (Scheme 4). These complexes were isolated in essentially quantitative yields by simply removing the solvent. The $^1H$ NMR spectrum of **7** as well as $^1H$ NMR and $^{31}P$ NMR spectra of the complex **6** showed only one set of signals, suggesting that only one isomer was obtained. The crystal structure of **5** evidenced an *anti* disposition of the pyridine and DMAP moieties. By analogy we propose the same geometry for **6** and **7** [13], as attempts to obtain single crystals of these compounds for X-ray diffraction studies were unsuccessful.

Metathetical reactions also occurred when complex **4** was treated with LiX (Scheme 5).

When $[Pt(DMSO)_2Cl_2]$ (DMSO = dimethylsulfoxide) was refluxed in ethanol with compound **1**, the monomeric platinum derivative **8** was obtained (Scheme 6).

The observation of a single SMe resonance at 3.61 ppm with $^{195}Pt$ satellites ($^3J_{Pt-H}$ = 25 Hz) as well as the finding in the IR spectrum of $\nu_{sS-O}$ at 1122 $cm^{-1}$ indicated an S-bonded DMSO configuration. Compound **8** was also fully characterized by X-ray diffraction.

Following with our aim to obtain new [N–C–M] systems we turned to N-protected indoles, expecting cyclometallation at C-3 to emerge. This strategy led us to synthesize cyclometallated complexes with a new metal-nitrogen bond and a new C–M bond with C-3 of the indole derivative. In fact 1-methyl-2-(2′-pyridinyl)-1*H*-indole ($L^2$) formed almost quantitatively Pd and Pt complexes in accordance to our expectation (Scheme 7).

The substituent at the nitrogen atom should protect it from chelation, but should not deactivate the indole nucleus towards the electrophilic attack by the metal.

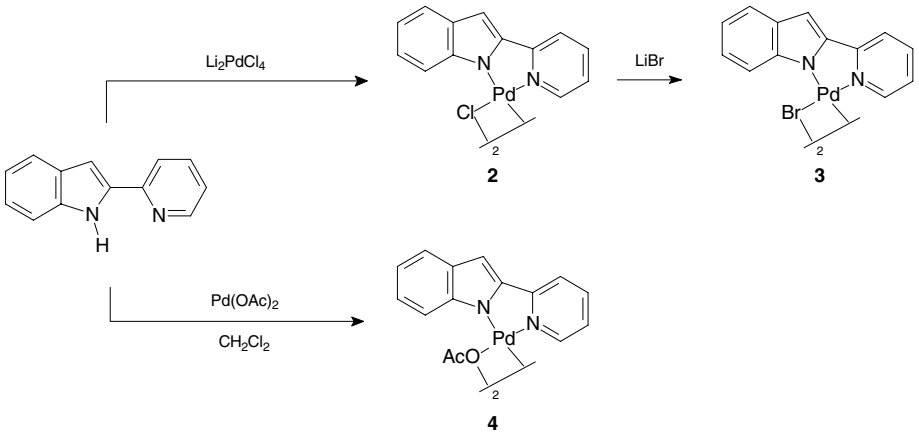


Scheme 3.

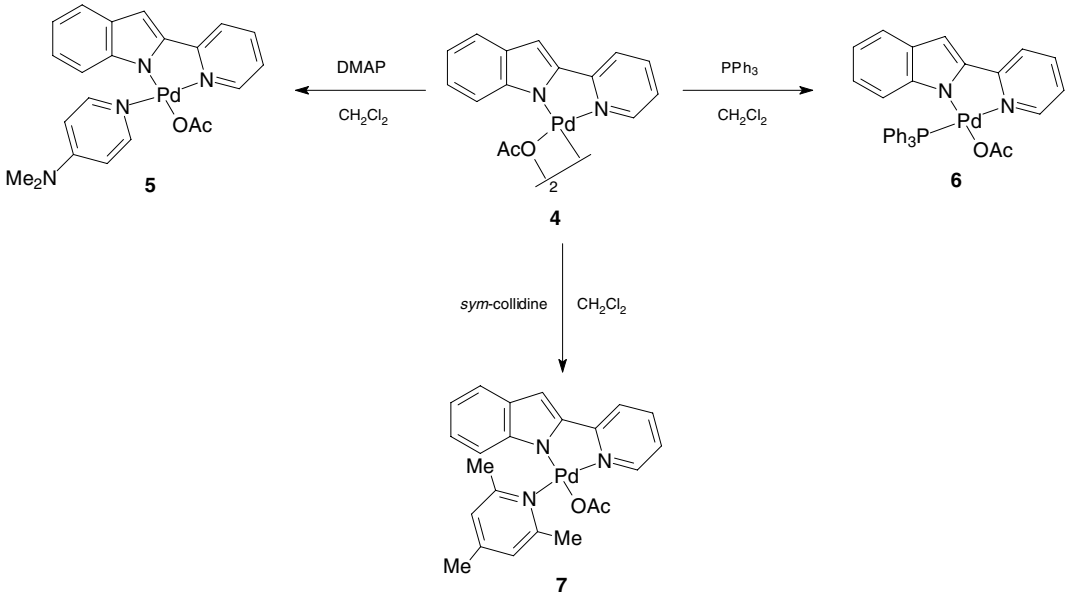


Scheme 4.

1-methyl-2-(2′-pyridinyl)-1*H*-indole ($L^2$) led to the synthesis of several cyclometallated palladium and platinum derivatives, whose reactivity was also investigated. Reaction with $Pd(OAc)_2$ in $CH_3CN$ yielded the dimeric, cyclopalladated product **9** (Scheme 8).

Strong bands were again observed at 1575 and 1417 $cm^{-1}$ due to the $\nu_{as(COO)}$ and $\nu_{s(COO)}$ stretching vibrations, respectively, and in the $^1H$ NMR spectrum a singlet at 2.33 ppm, characteristic of acetate bridging [13b]. The same reaction, when carried out with $Li_2PdCl_4$ in ethanol, even in presence of AcONa, gave product **10** (Scheme 9), for which $\nu_{(Pd-Cl)}$ occurred at 277 and 254 $cm^{-1}$.

Compound **10** was suspended in ethanol and carbon monoxide was bubbled through the reaction mixture at room temperature in the presence of $NEt_3$ as a proton scavenger. Metallic palladium separated out, while the organic ligand was recovered in good yield (73%) as 3-carbethoxy-1-methyl-2-(2′-pyridinyl)-1*H*-indole **11** (Scheme 10).

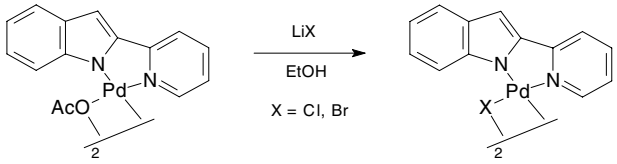


Scheme 5.

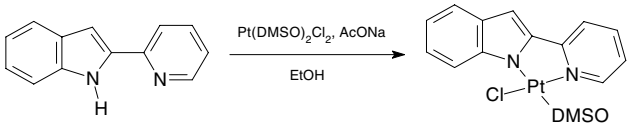


Scheme 6.

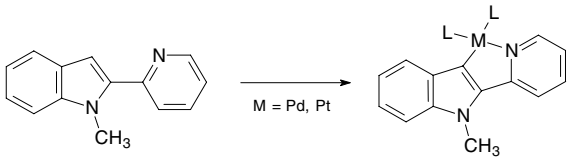


Scheme 7.

The functionalization of 1-methyl-2-(2′-pyridinyl)-1*H*-indole at C-3 of the indole moiety was readily achieved. Similar reactions, when conducted with secondary amines instead of ethanol, did not yield the corresponding carboxamide derivatives in a reproducible manner.

As reported by some of us [8] gramine and related compounds are good candidates and precursors for the formation of five- and six-membered indole-fused palladacycles and platinacycles. Subsequently, we investigated the possibility of obtaining other palladacycles and platinacycles by replacing the $NMe_2$ group with pyrazoles. The major isolated products from the reactions of gramine and pyrazoles are shown in Scheme 11. In this case six-membered rings were produced, their geometry being quite similar to that of tryptamine-like metallacycles reported in previous papers [6,9].

In order to obtain the same kind of product when the indole nitrogen is methylated, it is necessary to start from the corresponding gramine methiodide (Scheme 12).

Pyrazole and 3,5-dimethylpyrazole in the presence of $Pd(OAc)_2$ in $CH_2Cl_2$ gave different dimeric platina- and palladacycles as shown in Scheme 13, whereas working with $Pt(DMSO)_2Cl_2$ monomeric Pt complexes were obtained (Scheme 13).

In these instances new N–M–C bonds were formed, affording six-membered pallada- and platinacycles. These complexes, particularly the Pd ones, shall be

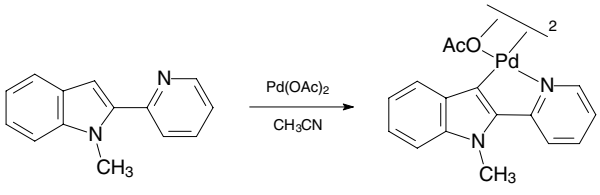


Scheme 8.

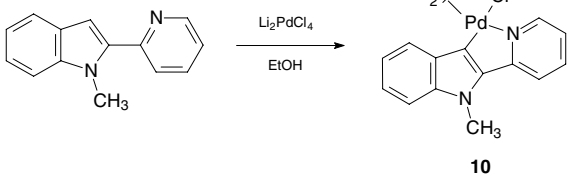


**10**

Scheme 9.

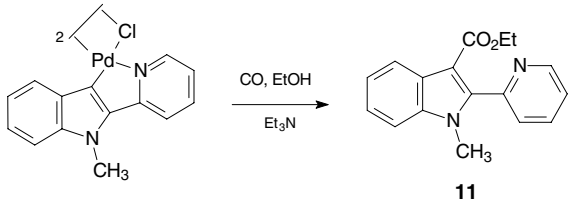


**11**

Scheme 10.

tested for catalytic activity in cross-coupling reactions, in order to discover whether they might mediate the formation of new C–C bonds. Complex **12** has also been characterized by X-ray diffraction.

### 1.1. Catalytic activity

Palladacycles have been thoroughly investigated as precatalysts in C–C bond formation reactions; one of the most popular cross-couplings is the Heck procedure. A wide variety of substrates has been used to design catalyst precursors endowed with good activity in cross-coupling reactions. As phosphapalladacycles [14] and phosphine-free N-heterocyclic carbenes are air- and moisture- sensitive they have to be handled under an inert atmosphere. Recently, carbothioamide-derived palladacycles were successfully used as precatalysts in Heck and Suzuki–Miyaura reactions [15]. Gladysz and coworker [16] introduced very active catalytic systems based on fluorous Schiff-bases palladacycle complexes as source of palladium nanoparticles having TON values exceeding one million. A new generation of air-stable and highly active Pd complexes for C–C and C–N coupling with aryl chlorides was introduced by Indolese and coworkers [17]. Other remarkable results were reported by Najera and coworkers [18] with oxime-derived palla-

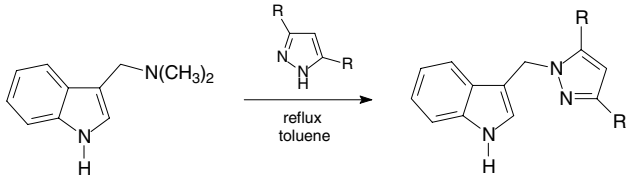


**HL[3]**: R = H
**HL[4]**: R = Me

Scheme 11.

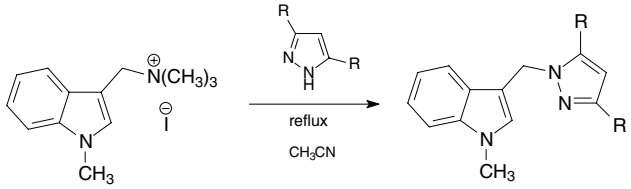


**HL[5]**: R = Me
**HL[6]**: R = H

Scheme 12.

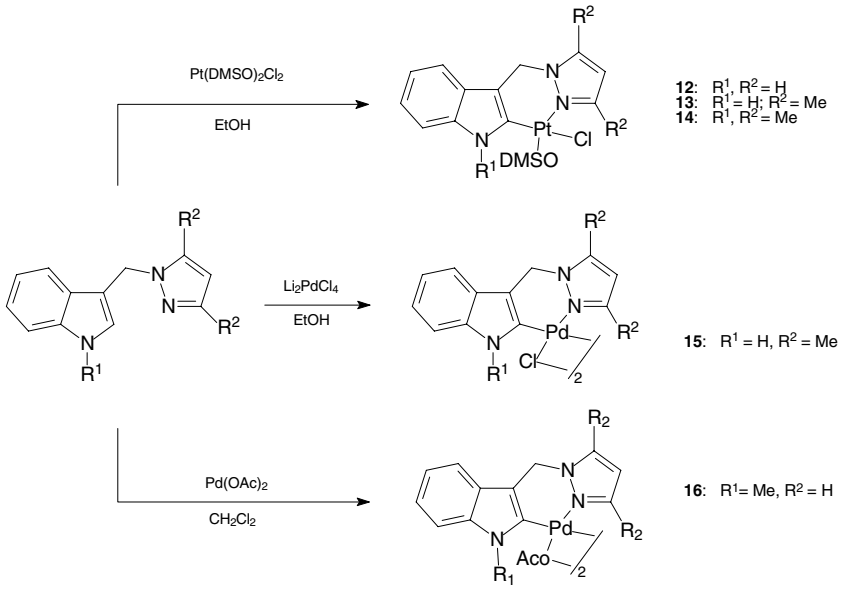


Scheme 13.

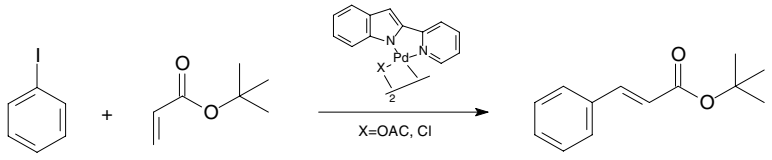


Scheme 14.

dacycles that are extremely active in Sonogashira and Glaser-type reactions. Other very active catalytic complexes were used in the Heck–Mizoroki reaction [19].

Starting with the well-defined and air-stable complexes **2** and **4**, we tested their performance as (pre)catalysts for the Heck cross-coupling reaction using iodobenzene and *tert*-butyl acrylate as the alkene (Scheme 14). In order to optimize reaction conditions, several combinations were tried of the two precatalysts, metal loadings, ligands, bases and solvents.

The use of THF or dioxane resulted in poor yields, that were improved when more polar solvents were employed, such as N-methylpyrrolidone (NMP) or DMF. Reaction conditions were subsequently optimized working in DMF at different temperatures (70, 90, 110 °C and at reflux). $K_3PO_4$, $Na_2CO_3$, $NBu_3$, $NEt_3$ were tried as bases. Even $PPh_3$ and $PCy_3$ were tested as additive ligands; some trials were carried out in the absence of any ligand.

Data in Table 1 show that the use of organic bases generally leads to higher yields for the coupling reaction. The difference in yields for a simple change of base is more marked for $K_3PO_4/Na_2CO_3$. **2** and **4**, used to generate in situ other complexes by interaction with either $Ph_3P$ or $Cy_3P$, proved catalytically active in the synthesis of (*E*)-*tert*-butyl cinnamate, albeit to different degree. The best results were obtained with in situ formed 1:1 **4**-$Cy_3P$ complex; the amount of this catalyst, initially tried at 5% molar, was subsequently lowered down to 0.1% without affecting the yield. In order to evaluate the stability of the catalytic system, after the reaction of iodobenzene and *tert*-butyl-acrylate was completed we made further additions of the reagents and verified the efficiency of the catalyst after each one. Four additions of PhI and acrylate were consecutively operated at the end of the catalytic cycle, and the uniformity of yields demonstrated the stability and persistent activity of **2** and **4**. For latter catalyst entries 13, 15, 17 and 19 in Table 1 report the yields found at the end of the last catalytic cycle. In preliminary work aimed to improve the values of TON and TOF, we found in some instances TON values close to 1,000,000. These experiments will be repeated and further optimized in the next future. In the reactions studied so far, preformed complex **6** showed the same catalytic activity as its precursors.

### 1.2. Structure of $C_{22}H_{22}N_4O_2Pd$ (**5**)

A view of compound **5** is shown in Fig. 1. Selected interatomic distances and angles are reported in Table 2. The coordination of the bidentate pyridinyl–indolyl

Table 1

| Entry | Catalyst | Base | Ligand | Solvent | $T$ (°C) | $t$ (h) | Yield (%) |
|---|---|---|---|---|---|---|---|
| 1 | **4** | – | – | DMF | 110 | 8 | 6 |
| 2 | **4** | $NEt_3$ | – | DMF | 110 | 14 | 16 |
| 3 | **4** | – | $PPh_3$ | DMF | 110 | 11 | 9 |
| 4 | **4** | $NEt_3$ | $PPh_3$ | THF | Reflux | 12 | 31 |
| 5 | **4** | $NEt_3$ | $PPh_3$ | Dioxane | Reflux | 8 | 47 |
| 6 | **4** | $NEt_3$ | $PPh_3$ | NMP | Reflux | 5 | 82 |
| 7 | **4** | $NEt_3$ | $PPh_3$ | DMF | 110 | 2.5 | 98 |
| 8 | **4** | $Na_2CO_3$ | $PPh_3$ | DMF | 110 | 7 | 22 |
| 9 | **4** | $K_3PO_4$ | $PPh_3$ | DMF | 110 | 8 | 14 |
| 10 | **4** | $NBu_3$ | $PPh_3$ | DMF | 110 | 5 | 88 |
| 11 | **4** | $NEt_3$ | $PPh_3$ | DMF | r.t. | 12 | 2 |
| 12 | **2** | $NEt_3$ | $PPh_3$ | DMF | 70 | 10 | 46 |
| 13 | **2** | $NEt_3$ | $PPh_3$ | DMF | 90 | 7 | 98 |
| 14 | **2** | $NEt_3$ | $PCy_3$ | DMF | 70 | 14 | 31 |
| 15 | **2** | $NEt_3$ | $PCy_3$ | DMF | 90 | 6 | 97 |
| 16 | **4** | $NEt_3$ | $PPh_3$ | DMF | 70 | 12 | 54 |
| 17 | **4** | $NEt_3$ | $PPh_3$ | DMF | 90 | 6 | 98 |
| 18 | **4** | $NEt_3$ | $PCy_3$ | DMF | 70 | 10 | 25 |
| 19 | **4** | $NEt_3$ | $PCy_3$ | DMF | 90 | 5 | 98 |

Reaction conditions: catalyst $5 \times 10^{-4}$ mmol, ligand $10^{-3}$ mmol, PhI 0.5 mmol, *tert*-butylacrylate 0.6 mmol, base 1.0 mmol in 3 ml of DMF.

ligand to the palladium atom occurs through the indole N(1) and the pyridine N(2) atoms, and gives rise to a pentatomic metallacycle. The square planar palladium atom completes its coordination sphere with an acetate anion, *trans* to the indole nitrogen, and with a 4-dimethylaminopyridine molecule, *trans* to the pyridinic nitrogen. The two Pd–N interactions are almost identical and comparable with the average Pt–N interaction in complex **8** (vide infra). The indole ligand lies essentially in the coordination plane, whereas the acetate and 4-dimethylaminopyridine ligands are almost perpendicular to it, as can be appreciated by the torsion angle N(1)–Pd–N(3)–C(18) of 98.0° and from the N(1)–Pd–O(1)–C(21) angle that is 92.4°. Such orientations are imposed by the need of minimising intramolecular contacts of these two ligands with the pyridinyl–indolyl ligand.

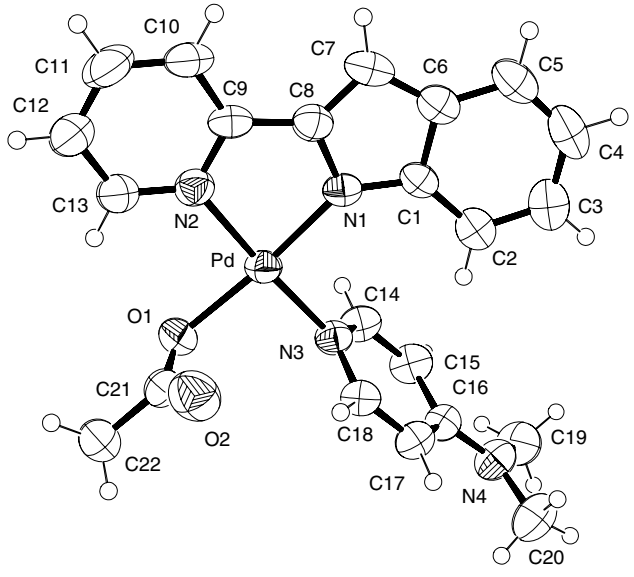


Fig. 1. ORTEP view of compound **5**. Thermal ellipsoids at 50% probability.

Table 2
Selected interatomic distances (Å) and angles (°) for compound **5**

| | |
|---|---|
| Pd–N(1) | 2.012(3) |
| Pd–N(2) | 2.021(3) |
| Pd–N(3) | 2.021(3) |
| Pd–O(1) | 2.035(2) |
| O(1)–C(21) | 1.293(5) |
| O(2)–C(21) | 1.219(5) |
| N(1)–C(1) | 1.371(4) |
| N(1)–C(8) | 1.382(4) |
| N(2)–C(13) | 1.341(5) |
| N(2)–C(9) | 1.358(4) |
| N(3)–C(18) | 1.345(4) |
| N(3)–C(14) | 1.346(4) |
| N(4)–C(16) | 1.341(4) |
| N(4)–C(19) | 1.447(5) |
| N(4)–C(20) | 1.460(5) |
| C(1)–C(6) | 1.430(5) |
| C(6)–C(7) | 1.403(5) |
| C(7)–C(8) | 1.374(5) |
| C(8)–C(9) | 1.444(5) |
| C(14)–C(15) | 1.367(5) |
| C(15)–C(16) | 1.412(5) |
| C(16)–C(17) | 1.402(5) |
| C(17)–C(18) | 1.357(5) |
| C(21)–C(22) | 1.509(5) |
| N(1)–Pd–N(2) | 81.14(12) |
| N(1)–Pd–N(3) | 95.67(12) |
| N(2)–Pd–N(3) | 176.54(12) |
| N(1)–Pd–O(1) | 174.80(11) |
| N(2)–Pd–O(1) | 93.66(12) |
| N(3)–Pd–O(1) | 89.52(12) |
| C(16)–N(4)–C(19) | 122.5(3) |
| C(16)–N(4)–C(20) | 121.4(3) |
| C(19)–N(4)–C(20) | 116.0(3) |

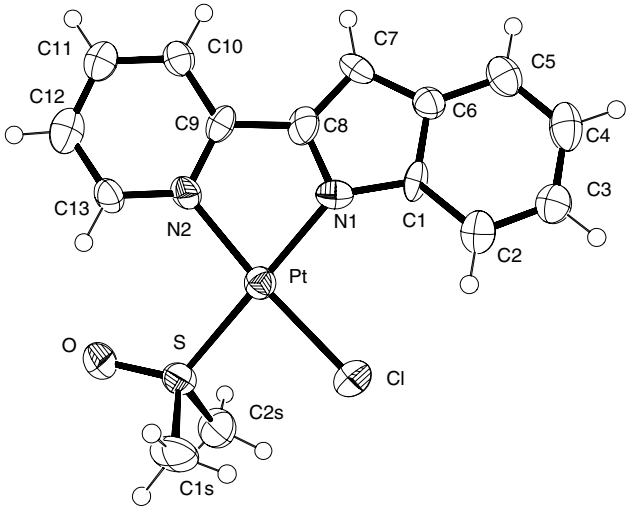


Fig. 2. ORTEP view of compound **8**. Thermal ellipsoids at 50% probability.

The aminic nitrogen atom N(4) displays a planar trigonal rather than a tetrahedral geometry, as predicted by the VSEPR theory, because the lone pair is not exclusively localised on the nitrogen atom but delocalised throughout the aromatic π system. As a consequence the N(4)–C(16) bond length of 1.341(4) Å is shorter than the expected value for a C($sp^2$)–N($sp^3$) interaction (1.395 Å). The whole aromatic system is also affected by the conjugation, with two distances, C(14)–C(15) and C(17)–C(18), significantly shorter.

### 1.3. Structure of $C_{15}H_{15}ClN_2OPtS$ (**8**)

A view of compound **8** is shown in Fig. 2. Selected interatomic distances and angles are reported in Table 3. The coordination of the bidentate pyridinyl–indolyl ligand to the platinum atom occurs in the same way as for the previous palladium complex. The square planar coordination of the metal is completed by a dimethylsulphoxyde (DMSO) molecule and a chloride ion, *trans* to the N(1) and N(2) atoms, respectively. Maximum deviation from the average coordination plane is observed for atom N(1) 0.165(8) Å; the torsion angle N(1)–C(8)–C(9)–N(2) is 6.3°.

The molecular structure of **8** can be compared with that of σ-{Pt[1*H*-indole-1-methyl-2-(2′pyridinil-$C^3$,$N^1$)]-(DMSO)Cl} [10], where the indolic moiety is metallated through the C(8) atom. The Pt–N(2) distance is statistically identical (within 3 times its e.s.d.) to that found in compound σ-{Pt[1*H*-indole-1-methyl-2-(2′pyridinil-$C^3$,$N^1$)]-(DMSO)Cl} and very close to the Pt–N(1) distance. The Pt–Cl interaction is here shorter due to different *trans* effect. Slightly different Pt–S distances are observed in the two compounds, probably owing to packing effects. All the rings of the pyridinyl–indolyl ligand are planar within the experimental error.

Table 3
Selected interatomic distances (Å) and angles (°) for compound **8**

| | |
|---|---|
| Pt–N(1) | 2.008(8) |
| Pt–N(2) | 2.043(8) |
| Pt–S | 2.234(3) |
| Pt–Cl | 2.300(3) |
| S–O | 1.478(7) |
| S–C(1S) | 1.776(10) |
| S–C(2S) | 1.778(10) |
| N(1)–C(8) | 1.359(12) |
| N(1)–C(1) | 1.415(11) |
| N(2)–C(9) | 1.350(12) |
| N(2)–C(13) | 1.341(11) |
| C(8)–C(9) | 1.451(13) |
| C(1)–C(6) | 1.411(14) |
| C(6)–C(7) | 1.405(13) |
| C(7)–C(8) | 1.384(13) |
| C(9)–C(10) | 1.394(13) |
| C(10)–C(11) | 1.377(13) |
| C(11)–C(12) | 1.374(14) |
| C(12)–C(13) | 1.381(14) |
| N(1)–Pt–N(2) | 80.1(3) |
| N(1)–Pt–S | 174.7(2) |
| N(1)–Pt–Cl | 95.0(2) |
| N(2)–Pt–S | 99.2(2) |
| N(2)–Pt–Cl | 175.1(2) |
| S–Pt–Cl | 85.72(10) |

### 1.4. Structure of $C_{14}H_{16}ClN_3OPtS$ (**12**)

The compound crystallizes with two independent molecules in the asymmetric unit.

Selected interatomic distances and angles are reported in Table 4. A perspective view of one of the two molecules is displayed in Fig. 3. Both molecules contain a square planar platinum atom coordinated by the indole ligand through one of the two atoms of the pyrazole moiety [N(11) or N(12)] and a carbon atom of the indole moiety [C(81) or C(82)]. A chloride anion, *trans* to the carbon atom C(81) [or C(82)], and a DMSO molecule, *trans* to N(11) [or N(12)], complete the coordination sphere. The six-membered metallacycle resulting from coordination of the pirazolylindolato ligand displays a boat-type conformation. The orientation of the DMSO molecule is determined by the presence of an intramolecular hydrogen bond between the DMSO oxygen and the indole nitrogen (Fig. 3) [ N(91)···O(1) 2.840(7) Å, N(91)–H(91)···O(1) 121.7(4)° for the first molecule; N(92)···O(2) 2.820(7) Å, N(92)–H(92)···O(2) 122.6(3)° for the second molecule]. The conformational and geometric parameters of both molecules are very similar. The possibility of having missed a symmetry relation between the two can be ruled out by inspection of the packing. If we consider the Pt···Pt contacts between adjacent molecules we realise that one of the two molecules displays only one Pt···Pt contact of 5.366(1) Å with related symmetry ($2-x$, $1-y$, $-z$) whereas the other molecule displays two Pt···Pt contacts of 4.891(1) and 4.953(1) Å with related

Table 4
Selected interatomic distances (Å) and angles (°) for compound **12**

| | |
|---|---|
| Pt(1)–C(81) | 1.987(6) |
| Pt(1)–N(11) | 2.050(5) |
| Pt(1)–S(1) | 2.205(1) |
| Pt(1)–Cl(1) | 2.397(2) |
| Pt(2)–C(82) | 1.986(5) |
| Pt(2)–N(12) | 2.055(4) |
| Pt(2)–S(2) | 2.206(1) |
| Pt(2)–Cl(2) | 2.397(2) |
| N(11)–C(21) | 1.347(8) |
| N(11)–N(51) | 1.353(6) |
| N(12)–C(22) | 1.344(7) |
| N(12)–N(52) | 1.349(6) |
| N(51)–C(41) | 1.349(7) |
| N(51)–C(61) | 1.466(7) |
| N(52)–C(42) | 1.337(7) |
| N(52)–C(62) | 1.460(7) |
| N(91)–C(101) | 1.354(7) |
| N(91)–C(81) | 1.387(7) |
| N(92)–C(102) | 1.381(7) |
| N(92)–C(82) | 1.385(6) |
| C(21)–C(31) | 1.373(9) |
| C(22)–C(32) | 1.384(9) |
| C(31)–C(41) | 1.362(9) |
| C(32)–C(42) | 1.397(10) |
| C(61)–C(71) | 1.496(8) |
| C(62)–C(72) | 1.494(7) |
| C(71)–C(81) | 1.381(7) |
| C(71)–C(111) | 1.427(7) |
| C(72)–C(82) | 1.392(7) |
| C(72)–C(112) | 1.434(7) |
| C(101)–C(111) | 1.418(7) |
| C(102)–C(112) | 1.413(7) |
| C(81)–Pt(1)–N(11) | 86.2(2) |
| C(81)–Pt(1)–S(1) | 94.8(2) |
| N(11)–Pt(1)–S(1) | 176.7(1) |
| C(81)–Pt(1)–Cl(1) | 173.0(2) |
| N(11)–Pt(1)–Cl(1) | 88.5(1) |
| S(1)–Pt(1)–Cl(1) | 90.71(6) |
| C(82)–Pt(2)–N(12) | 85.8(2) |
| C(82)–Pt(2)–S(2) | 94.7(2) |
| N(12)–Pt(2)–S(2) | 177.4(1) |
| C(82)–Pt(2)–Cl(2) | 173.2(2) |
| N(12)–Pt(2)–Cl(2) | 89.0(1) |
| S(2)–Pt(2)–Cl(2) | 90.68(5) |

symmetries $(2 - x, -y, -1 - z)$ and $(1 - x, -y, -1 - z)$, respectively.

## 2. Experimental

Elemental analyses were carried out on a Perkin–Elmer 2400 (series II) elemental analyzer. The IR spectra in the 4000–200 $cm^{-1}$ region were performed on KBr pellets on a Perkin–Elmer 283 spectrophotometer. The $^{1}H$, $^{13}C$ and $^{31}P$ NMR spectra were obtained for solution in $CDCl_3$ or DMSO-$d_6$ and were recorded on a Bruker Avance 400 spectrometer. Electron-impact mass spectra (EI-MS) were obtained on a VG 7070(EQ) instrument.

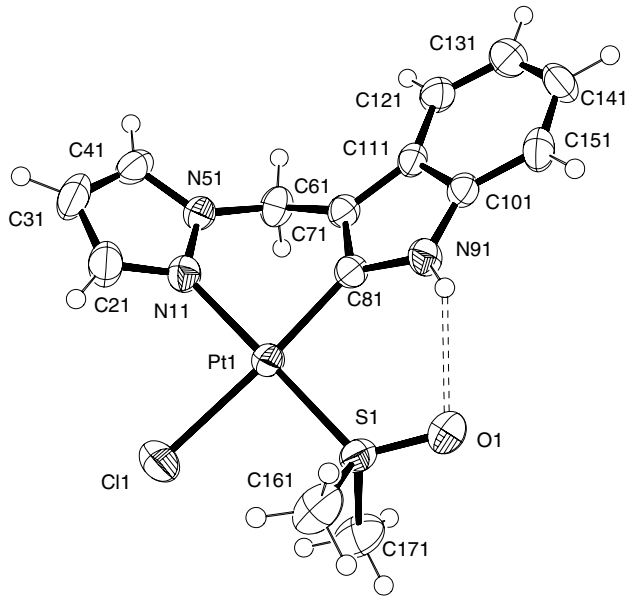


Fig. 3. ORTEP view of one of the two independent molecules of compound **12**. Thermal ellipsoids at 50% probability.

### 2.1. Compound *2*

Brown-orange solid: m.p. 263 °C (dec.) ; $^{1}H$ NMR ($CDCl_3$, ppm): 6.46 (s, 2H), 8.10–6.70 (m, 16 H); $^{13}C$ NMR ($CDCl_3$, ppm): 101.87, 113.51, 118.32, 119.15, 121.10, 122.24, 128.81, 132.41, 136.56, 145.02, 145.41, 152.51, 156.52. Elemental analysis (%): Calc.: C 46.60, H 2.71, N 8.36. Found: C 46.91, H 3.02, N 8.17; IR: 307, 294 $cm^{-1}$.

### 2.2. Compound *3*

Brown-orange solid: m.p. 270 °C (dec.); $^{1}H$ NMR ($CDCl_3$, ppm): 6.45 (s, 2H), 8.15–6.85 (m, 16 H); $^{13}C$ NMR ($CDCl_3$, ppm): 101.85, 112.93, 118.23, 119.53, 121.02, 123.10, 128.51, 134.53, 136.82, 144.81, 145.23, 152.21, 156.13. Elemental analysis (%): Calc.: C 41.14, H 2.39, N 7.38. Found: C 41.05, H 2.41, N 7.65.

### 2.3. Compound *4*

Brown-orange solid: m.p. 255 °C (dec.); IR: 1572, 1412 $cm^{-1}$, $^{1}H$ NMR ($CDCl_3$, ppm): 2.35 (s, 6H), 6.41 (s, 2H); 8.20–6.75 (m, 16 H); $^{13}C$ NMR ($CDCl_3$, ppm): 24.16, 101.37, 113.37, 118.10, 119.03, 121.25, 122.11, 128.65, 129.76, 136.76, 144.92, 145.22, 152.41, 156.43, 185.13. Elemental analysis (%): Calc.: C 50.23, H 3.37, N 7.81. Found: C 50.15, H 3.31, N 7.67.

### 2.4. Compound *5*

$^{1}H$ NMR ($CDCl_3$, ppm): 2.03 (s, 3H), 3.12 (s, 6H), 5.73 (d, 1H), 6.58 (d, 2H), 6.72 (t, 1H), 6.97 (s, 1H),

7.01 (t, 1H), 7.01 (t, 1H), 7.52 (d, 1H), 7.66 (d, 1H), 7.70 (t, 1H), 8.03 (d, 1H), 8.53 (d, 2H).

### 2.5. Compound **6**

$^1$H NMR ($CDCl_3$, ppm): 1.94 (s, 3H), 6.04 (d, 1H), 6.61 (t, 1H), 6.98 (t, 1H), 7.08 (s, 1H), 7.13 (t, 1H), 7.39 (d, 1H), 7.41–7.67 (m, 15H), 7.77 (t, 1H), 7.82 (d, 1H), 8.15 (d, 1H); $^{31}$P NMR ($CDCl_3$, ppm): 30.30 (s).

### 2.6. Compound *7*

$^1$H NMR ($CDCl_3$, ppm): 1.97 (s, 3H), 2.46 (s, 3H), 3.45 (s, 6H), 5.40 (t, 1H), 6.32 (d, 1H), 6.96 (s, 1H), 7.05 (t, 1H), 7.11 (s, 2H), 7.41 (t, 1H), 7.53 (d, 1H), 7.66 (t, 1H), 7.74 (d, 1H), 8.08 (d, 1H).

### 2.7. Compound **8**

Orange solid: m.p. 147–148 °C; IR: 1122, 328 cm$^{-1}$; $^1$H NMR ($CDCl_3$, ppm): 3.61 (s, 6H, $J_{H-Pt}$ = 25Hz), 6.95 (s, 1H); 7.00–8.70 (m, 7H), 9.49 (d, 1H, $J$ = 5.8 Hz; $J_{H-Pt}$ = 43 Hz); $^{13}$C NMR ($CDCl_3$, ppm): 44.6 ($J_{Pt-CH_3-S}$ = 44 Hz), 104.17, 116.41, 119.00, 118.85, 120.51, 121.20, 129.51, 130.02, 138.61, 146.32, 147.91, 148.21 ($J_{Pt-C6'}$ = 40 Hz), 158.13. Elemental analysis (%): Calc.: C 35.90, H 3.01, N 5.58. Found: C 35.83, H 3.15, N 5.71.

### 2.8. Compound **9**

Orange solid: m.p. 193–195 °C; IR: 1575, 1417 cm$^{-1}$; $^1$H NMR ($CDCl_3$, ppm): 2.33 (s, 6H), 3.62 (s, 6H); 7.85–6.65 (m, 16 H); $^{13}$C NMR ($CDCl_3$, ppm): 24.21, 32.11, 110.23, 120.13, 125.01, 125.63, 127.31, 139.02, 138.04, 141.46, 142.00, 150.93, 153.97, 155.23; Elemental analysis (%): Calc.: C 51.56, H 3.79, N 7.52. Found: C 51.45, H 3.57, N 7.59.

### 2.9. Compound **10**

Brown-orange solid: m.p. 205–207 °C; IR: 277, 254 cm$^{-1}$. Elemental analysis (%): Calc.: C 48.16, H 3.18, N 8.02. Found: C 47.79, H 3.33, N 7.91%.

### 2.10. Compound **11**

$^1$H NMR ($CDCl_3$, ppm): 1.22 (t, 3H, $J$ = 6.8 Hz), 3.65 (s, 3H), 4.22 (q, 2H, $J$ = 6.8 Hz), 7.11–7.34 (m, 4H,), 7.38 (d, 1H), 7.83 (d, 1H), 8.28 (d, 1H) 8.77 (d, 1H). MS (EI) (70 eV) *m*/*z*: 280, 235, 207.

### 2.11. Compound **12**

Brown solid: m.p. 174 °C (dec.); $^1$H NMR ($CDCl_3$, ppm): 3.67 (t, 6H), 5.52 (s, 2H), 6.44 (t, 1H), 7.05 (m, 2H), 7.35 (dd, 1H), 7.43 (d, 1H), 7.69 (d, 1H), 8.42 (d, 1H), 9.89 (s, 1H); $^{13}$C NMR ($CDCl_3$, ppm): 46.91, 49.52, 105.31, 106.64, 111.37, 115.65, 119.32, 120.33, 122.91, 126.62, 132.71, 136.93, 143.77.

### 2.12. Compound **13**

Brown solid: m.p. 159 °C (dec.); $^1$H NMR ($CDCl_3$, ppm): 2.41 (s, 3H), 2.60 (s 3H), 3.56 (s, 6H), 5.28 (s, 2H), 5.96 (s, 1H), 6.90 (t, 1H), 7.05 (t, 1H), 7.34 (d, 1H), 7.41 (d, 1H), 9.39 (s, 1H). $^{13}$C NMR (DMSO, ppm): 12.22, 15.83, 41.31, 45.74, 107.79, 108.02, 115.50, 116.13, 118.92, 119.22, 127.04, 128.33, 137.48, 142.35, 151.19.

### 2.13. Compound **14**

Pale yellow solid: m.p. 125 °C (dec.); $^1$H NMR ($CDCl_3$, ppm): 3.91 (s, 3H), 7.26 (s, 1H), 7.02 (m, 2H), 7.37 (d, 1H), 5.19 (d, 1H), 5.51 (d, 1H), 5.86 (s, 1H), 2.36 (s, 3H), 2.50 (s, 3H), 3.50 (t, 3H), 3.68 (t, 3H); $^{13}$C NMR ($CDCl_3$, ppm): 12.23, 15.35, 35.71, 45.53, 46.18, 47.25, 107.23, 107.92, 109.79, 115.28, 119.02, 119.36, 127.09, 135.54, 138.78, 141.02, 151.34.

### 2.14. Compound **15**

Orange solid: m.p. 270 °C (dec.). Elemental analysis (%): Calc.: C 45.92, H 3.85, N 11.48. Found: C 45.79, H 3.90, N 11.08.

### 2.15. Compound **16**

$^1$H NMR ($CDCl_3$, ppm): 1.27 (s, 6H), 3.15 (s, 6H), 4.43 (d, 2H), 6.08 (d, 2H), 6.28 (d, 2H), 6.55 (s, 2H), 7.07 (t, 2H), 7.14 (d, 2H), 7.23 (t, 2H), 7.80 (s, 2H), 7.82 (s, 2H); $^{13}$C NMR ($CDCl_3$, ppm): 30.12, 32.15, 36.32, 76.29, 107.85, 110.82, 120.44, 124.61, 129.67, 132.82, 139.25, 140.74, 142.78, 143.51, 197.63.

## 3. X-ray structure determination

Numbers given in the X-Ray structures are only for crystallographic purpose and are not relevant to the nomenclature of heterocyclic compounds and metal-heterocyclic complexes.

*Crystal data for $C_{22}H_{22}N_4O_2Pd$ (**5**)*, f.w. 480.84, monoclinic, space group $P2_1/n$, (no. 14), $a$ = 14.8019(11), $b$ = 8.4800(6), $c$ = 16.4163(12) Å, $\beta$ = 96.75(1)°, $U$ = 2046.3(3) Å$^3$, $Z$ = 4, $d_{calc}$ = 1.561 Mg m$^{-3}$, $\mu$ = 0.932 mm$^{-1}$, $F$(0 0 0) 976, $R$ = 0.035, $wR_2$ = 0.072 on 2587 reflections with $I > 2\sigma(I)$. 15,861 Intensity data (3914 unique) were measured at room temperature on a Bruker Smart CCD diffractometer

with graphite monochromatized Mo Kα radiation ($\lambda = 0.71073$ Å). An empirical absorption correction (SADABS) [20] was applied to the data.

*Crystal data for $C_{15}H_{15}ClN_2OPtS$ (**8**),* f.w. 501.89, monoclinic, space group $P2_1/n$, (no. 14), $a = 5.884(3)$, $b = 14.855(5)$, $c = 17.616(6)$ Å, $\beta = 97.59(4)°$, $U = 1526(1)$ Å$^3$, $Z = 4$, $d_{calc} = 2.184$ Mg m$^{-3}$, $\mu = 9.500$ mm$^{-1}$, $F(0\,0\,0)$ 952, $R = 0.034$, $wR_2 = 0.074$ on 1644 reflections with $I > 2\sigma(I)$. 2985 intensity data (2659 unique) were measured at room temperature on a Enraf-Nonius CAD-4 diffractometer with graphite monochromatized Mo Kα radiation ($\lambda = 0.71073$ Å). Data were corrected for absorption using the psi-scan procedure [21].

*Crystal data for $C_{14}H_{16}ClN_3OPtS$ (**12**)*, f.w. 504.90, triclinic, space group $P\bar{1}$, (no. 2), $a = 9.8294(7)$, $b = 10.6651(8)$, $c = 15.3319(12)$ Å, $\alpha = 83.96(1)°$, $\beta = 82.17(1)°$, $\gamma = 79.88(1)°$, $U = 1562.1(2)$ Å$^3$, $Z = 4$, $d_{calc} = 2.147$ Mg m$^{-3}$, $\mu = 9.288$ mm$^{-1}$, $F(0\,0\,0)$ 960, $R = 0.024$, $wR_2 = 0.066$ on 5082 reflections with $I > 2\sigma(I)$. 14,168 Intensity data (5972 unique) were measured at room temperature on a Bruker Smart CCD diffractometer with graphite monochromatized Mo Kα radiation ($\lambda = 0.71073$ Å). An empirical absorption correction (SADABS) [20] was applied to the data. All structures were solved by Patterson and Fourier methods and refined on $F^2$ using SHELX-97 [22]. Non-hydrogen atoms were refined with anisotropic thermal parameters. Hydrogen atoms were experimentally observed and allowed to ride on the pertinent atoms.

## 4. Supplementary material

Full crystallographic data for compounds **5**, **8** and **12** have been deposited with the Cambridge Crystallographic Data Centre, CCDC 101098, 253707 and 253708. Copy may be obtained free of charge from the Director CCDC, 12 Union Road, Cambridge CB2 1EZ, UK (fax: +44 1223 336 033; e-mail: deposit@ccdc.cam.ac.uk).

## Acknowledgements

We thank Professor Cenini for helpful discussion. The present work was supported (PRIN 2003) by the Italian Ministero dell'Istruzione Università e Ricerca (MIUR).

## References

[1] J.P. Kleiman, M. Dubeck, J. Am. Chem. Soc. 65 (1963) 1544, for exhaustive reviews see also:;
(a) M.I. Bruce, Angew. Chem. Int. Ed. 16 (1977) 75;
(b) A.D. Ryabov, Synthesis (1985) 933;
(c) V.V. Dunina, O.A. Zalevskaja, V.M. Potapov, Russ. Chem. Rev. 57 (1988) 250;
(d) A.D. Ryabov, R. Van Eldik, G. Le Borgne, M. Pfeffer, Organometallics 12 (1993) 138.
[2] (a) M. Albrecht, G. Van Koten, Angew. Chem. Int. Ed. 40 (2001) 3750;
(b) J.M. Pollino, M. Weck, Synthesis (2002) 1277.
[3] (a) J. Vicente, I. Saura-Llames, P.G. Jones, Dalton Trans. (1993) 3619;
(b) G. Zhao, Q.G. Wang, T.C.W. Mak, Dalton Trans. (1998) 1241.
[4] R. Ares, M. López-Torres, A. Fernández, S. Castro-Juiz, Polyhedron 21 (2002) 2309.
[5] F. Basuli, P. Chattopadhyay, C. Sinha, Polyhedron 15 (1996) 2439.
[6] S. Tollari, S. Cenini, C. Tunice, G. Palmisano, Inorg. Chim. Acta 272 (1998) 18.
[7] S. Tollari, G. Palmisano, F. Demartin, M. Grassi, S. Magnaghi, S. Cenini, J. Organomet. Chem. 488 (1995) 79.
[8] S. Tollari, F. Demartin, S. Cenini, G. Palmisano, P. Raimondi, J. Organomet. Chem. 527 (1997) 93.
[9] R. Annunziata, S. Cenini, F. Demartin, G. Palmisano, S. Tollari, J. Organomet. Chem. 496 (1995) C1.
[10] S. Tollari, S. Cenini, A. Penoni, G. Granata, G. Palmisano, F. Demartin, J. Organomet. Chem. 608 (2000) 34.
[11] C. Crotti, S. Cenini, B. Rindone, S. Tollari, F. Demartin, J. Chem. Soc., Chem. Commun. (1986) 784.
[12] (a) R.P. Thummel, W. Hegde, J. Org. Chem. 54 (1989) 1720;
(b) F. Wu, J. Hardesty, R.P. Thummel, J. Org. Chem. 63 (1998) 4055;
(c) F. Wu, C.M. Chamchoumis, R.P. Thummel, Inorg. Chem. 39 (2000) 584.
[13] (a) G.K. Anderson, R.J. Cross, Chem. Soc. Rev. 9 (1980) 185;
(b) J. Vicente, M.C. Lagunas, E. Bleuel, M.C. Ramirez de Arellano, J. Organomet. Chem. 648 (2002) 62.
[14] J.M. Brunel, M.-H. Hirlemann, A. Heumann, G. Buono, Chem. Commun. (2000) 1869.
[15] Z. Xiong, N. Wang, M. Dai, A. Li, J. Chen, Z. Yang, Org. Lett. 6 (2004) 3337.
[16] C. Rocaboy, J.A. Gladysz, Org. Lett. 4 (2002) 1993.
[17] A. Schnyder, A.F. Indolese, M. Studer, H.-U. Blaser, Angew. Chem. Int. Ed. 41 (2002) 3668.
[18] D.A. Alonso, C. Najera, M.C. Pacheco, Adv. Synth. Catal. 345 (2003) 1146.
[19] (a) C.-A. Lin, F.-T. Luo, Tetrahedron Lett. 44 (2003) 7565;
(b) C.-T. Chen, Y.-S. Chan, Y.-R. Tzeng, M.-T. Chen, Dalton Trans. (2004) 2691.
[20] SADABS Area-Detector Absorption Correction Program, Bruker AXS, Inc. Madison, WI, USA, 2000.
[21] A.C.T. North, D.C. Phillips, F.S. Mathews, Acta Crystallogr. A 24 (1968) 351.
[22] G.M. Sheldrick, SHELXL-93-97, Universität Göttingen, Germany, 1997.